Single-point statistical moments of the nonhomogeneous stochastic advection equation in the small displacement limit

*

(Dated: November 1, 2026)

We derive closed-form expressions for the first four single-point statistical moments of the solution to a nonhomogeneous stochastic advection equation with a linear relaxation. While analytical solutions exist for homogeneous systems, nonhomogeneous cases have traditionally relied on intensive numerical simulations. Here, we investigate an analytical framework in a nonhomogeneous case. To include memory effects, we preserve a nonzero correlation time by treating the Gaussian transport velocity field as a piecewise-constant stochastic process. Using the method of characteristics, we solve the advection equation analytically and derive explicit and simple algebraic expressions for its moments in the small displacement limit as functions of the velocity field's variance and correlation time, relaxation time, and the mean state of the field. Our results show that variance and excess kurtosis scale linearly with both the correlation and relaxation timescales, while skewness is proportional to the square root of their product. The analytical results are validated against numerical simulations, demonstrating excellent agreement across a range of physical parameters. The resulting theory acts as a generalized "equation-of-state" style approach for predicting variability and non-Gaussian statistical behavior directly from the macroscopic mean state, providing potential applicability across transport systems with a wide range of length scales and correlation time scales, such as planetary atmospheres and porous media flows.

I. INTRODUCTION

[PAY ATTENTION TO DEFINITION OF EACH VARIABLE]The advection equation is a fundamental tool for characterizing the transport of physical quantities within fluid media. It is widely utilized to model tracer transport such as advection of chemical concentration in porous media [1–3], the evolution of scalar fields such as temperature [4], humidity [5], and pollutant concentrations [6, 7] in the high-Péclet-number regimes where diffusion effects become negligible. Due to its importance, methods to solve the advection equation in various conditions have been researched [8, 9].

While certain physical systems are adequately described by deterministic velocity fields, others are more accurately represented by stochastic transport velocities. In geology and hydrology, the advection equation with a random velocity field describes solute transport with random permeabilities in porous media [10–13]. In atmospheric sciences, it describes transport of passive scalars such as temperature in highly turbulent regions [14–16]. On astrophysical scales, similar stochastic ideas can be applied to model the propagation of cosmic rays, where the turbulent magnetic fields induce random particle trajectories [17, 18].

Consequently, significant efforts have been directed toward understanding the advection of physical quantities with random velocity fields to understand the statistical properties of the resulting solutions. Following Kolmogorov's work [19], Kraichnan [20] applied the idea of structure functions to passive scalars advected by random velocity fields to calculate anomalous scaling of structure functions. Subsequent work has refined Kraichnan's theory by calculating more precise scaling exponents [21], consideration of a finite correlation time [22], and combining the theory with Taylor's frozen-flow model [23]. Dynamical considerations have been investigated through equations of motion with an additive random forcing term to calculate the system's PDF via the Langevin and Fokker-Planck frameworks [24], as well as through direct approaches to solving the homogeneous advection equation with random velocity fields [25–28].

Although these previous studies have significantly advanced the stochastic transport theory, their analytical frameworks focused primarily on homogeneous advection equations [25–28] or on multi-point observables, most notably structure functions [20–23]. While structure functions are effective for determining scale-invariant properties by calculating the moments of the spatial difference of a field, they do not contain information about statistical moments at a fixed location. However, tracking these local single-point statistics is fundamental for characterizing the emergence of a non-Gaussian extreme probability distribution of the field. Understanding these local statistical properties is essential for calculating the probability of rare events of any tracer quantity in highly fluctuating media, such as turbulent atmospheres or porous media. Consequently, in the absence of a tractable analytical framework for the nonhomogeneous case, calculations of single-point moments have historically depended on numerical simulations [14, 29].

In this study, we present a fully analytical framework for calculating the single-point statistical moments of the solution of the nonhomogeneous advection equation subject to linear relaxation and stochastic transport with finite memory effects, where the linear relaxation mechanism models a continuous source and sink that drives the field back toward its spatial equilibrium profile. While this formulation relies on a specific forcing term, lin-

*

ear relaxation is a reasonable approximation in diverse transport applications. Establishing analytical solutions for this particular case therefore provides a theoretical benchmark for nonhomogeneous stochastic advection problems. To derive closed-form expressions, we adopt two idealized assumptions: first, to preserve fluid memory effects, instead of invoking the standard white-noise limit, the Gaussian velocity field is treated as a piecewise-constant stochastic process in time; second, the system is in the small displacement limit, where the characteristic distance traveled by the fluid within the velocity correlation time is small compared to the characteristic length scale of the spatial change of the field (i.e., the fluid does not see the change in the field within the velocity correlation time scale). Under these constraints, we derive closed-form expressions of the single-point statistical moments that depend solely on the variance and the correlation time of the Gaussian velocity field, the relaxation time, and the mean state of the field. By connecting moments with the mean profile with closed-form expressions, our framework provides a highly efficient alternative to traditional numerical simulations. In doing so, this work extends the analytical framework previously restricted to homogeneous systems into a nonhomogeneous case. These analytical expressions establish an "equation-of-state" style approach for the transport system, directly mapping microscopic temporal variability (the localized statistical moments) onto macroscopic spatial structure (the mean profile and its derivatives), while accounting for the finite memory effects of the velocity field.

II. MODEL SETUP

A. Stochastic Advection Equation and Its Exact Solution

Let us consider a one-dimensional fluid that transports a field $u(x,t)$ that is a function of position x and time t, where the transport of $u(x,t)$ occurs stochastically due to a random velocity field $v(t)$ while approaching an equilibrium profile u_e over time. As an idealized approximation of this process, we use a one-dimensional stochastic advection equation with linear relaxation:

$$\frac{\partial u(x,t)}{\partial t} + v(t)\frac{\partial u(x,t)}{\partial x} = -\frac{u(x,t)-u_e(x)}{\tau}, \tag{1}$$

where τ is the characteristic timescale of the linear relaxation, $u_e(x)$ is assumed to be a smooth function that depends only on x, and $v(t)$ is a Gaussian noise that depends only on t.

We solve Eq. (1) via the method of characteristics, as was done by [30] in the homogeneous case. Parameterizing the system with r and s, the characteristic equations of Eq. (1) are

$$\frac{dt}{dr} = 1 \tag{2}$$

$$\frac{dx}{dr} = v(r) \tag{3}$$

$$\frac{du}{dr} = -\frac{u-u_e(x)}{\tau}. \tag{4}$$

With the initial conditions $t(0)=0$, $x(0)=s$, and $u(0,s)=u_i(s)$, we obtain

$$r = t \tag{5}$$

$$x = s + \Delta s(r) \tag{6}$$

$$\Delta s(r) = \textstyle\int_0^r v(r')dr' \quad , \tag{7}$$

$$\begin{aligned} u(r,s) &= u_i(s)e^{-r/\tau} \\ &+ e^{-r/\tau}\frac{1}{\tau}\int_0^r u_e(s+\Delta s(r'))e^{r'/\tau}dr'. \end{aligned} \tag{8}$$

Since $u_e(s)$ is differentiable with respect to s and $\Delta s(r')$ is differentiable in r', we now rewrite Eq. (8) with integration by parts:

$$\begin{aligned} u(r,s) &= u_i(s)e^{-r/\tau} + u_e(s+\Delta s) - u_e(s)e^{-r/\tau} \\ &- e^{-r/\tau}\int_0^r \frac{\partial u_e}{\partial s}(s+\Delta s(r'))v(r')e^{r'/\tau}dr'. \end{aligned} \tag{9}$$

To find its steady-state solution, we pick r large enough that $(u_i(s)-u_e(s))e^{-r/\tau} \ll u_e(s+\Delta s)$ for all s. For this to be true with any finite $u_i(s)$, we must have $\tau \ll r$ (hence $\tau \ll t$), which we set as an assumption of our model. Then Eq. (9) approaches

$$\begin{aligned} u(r,s) &= u_e(s+\Delta s) \\ &- e^{-r/\tau}\int_0^r \frac{\partial u_e}{\partial s}(s+\Delta s(r'))v(r')e^{r'/\tau}dr', \end{aligned} \tag{10}$$

which is clearly independent of the initial condition (and coincides with the exact solution when $u(0,s)=u_e(s)$ is used as the initial condition).

Equation (10), along with Eq. (5)–(6), provides the exact steady-state solution to Eq. (1) for any velocity field $v(t)$ regardless of the initial condition. However, calculating the statistical moments of $u(t,x)$ in this general form remains analytically intractable due to the complexity of the integral.

B. Asymptotic Expansion and Noise Discretization

To obtain a closed-form solution or the statistical moments of $u(t,x)$, we model the noise $v(t)$ as a piecewise-constant, stationary Gaussian process. Specifically, $v(t)$ takes a random value sampled from a time-invariant Gaussian distribution over successive intervals of duration $\Delta t \ll t$. Because the mean and the variance of $v(t)$

remain constant over time, the system's steady-state condition is preserved. This conceptually represents a staircase with random step heights in time, given by

$$v(t) = \sum_i v_i \left(H(t-t_i) - H(t-(t_i+\Delta t))\right), \quad (11)$$

where $v_i \sim \mathcal{N}(0, \sigma_v^2)$, v_i and v_j are uncorrelated if $i \neq j$, and $H(x)$ is a Heaviside step function. Here, Δt represents the finite velocity correlation time scale. Instead of the standard continuous framework where velocity correlation decays exponentially, the memory effect enters the model discretely: the velocity $v(t)$ remains constant over a duration Δt and completely uncorrelated across other intervals, yielding a piecewise-constant autocorrelation function. From now on, we shall call each step of such 'stairs' a time step for convenience. In this study, we consider only the case where the fluid does not 'see' the curvature of u_e and that of its spatial derivatives during its travel within the velocity correlation time Δt; namely, when he length scale of the spatial change in the n^{th} derivative of the equilibrium profile is much larger than the typical distance the fluid moves within the timescale of the noise Δt:

$$v(t)\Delta t \ll \frac{d^n u_e(x)/dx^n}{d^{n+1}u_e(x)/dx^{n+1}},\ n = 0, 1, 2, \ldots, \quad (12a)$$

or equivalently,

$$\delta_n := \frac{v(t)\Delta t}{\frac{d^n u_e(x)/dx^n}{d^{n+1}u_e(x)/dx^{n+1}}} \ll 1,\ n = 0, 1, 2, \ldots \quad (12b)$$

on average. This is a regime applicable to physical systems such as Earth's atmospheres [31–35]. The cases where the validity of (12a) brakes down include regions with an abrupt change in the equilibrium field u_e and the case where the distance traveled by the fluid within one correlation time $v(t)\Delta t$ is large due to high velocity or long fluid memory effects. Note that this criteria is satisfied when the denominator of the right side of (12a) is zero, and not satisfied when the numerator is zero. This also means if $d^n u/dx^n = 0$ for some n and $d^{n+1}u/dx^{n+1} \neq 0$, then (12a) is guaranteed not to be satisfied. In a physical system, $d^n u/dx^n$ is most likely to be not exactly zero, and the necessary condition is that all higher-order terms in the expansion are small compared to the leading-order terms. However, we will use a more restrictive condition (12a) to simplify our discussion.

Utilizing this limit, we expand $\partial u_e/\partial s(s+\Delta s)$ in the integrand in Eq.(10) about s:

$$\begin{aligned} u(r,s) &= u_e(s+\Delta s) - u_e'(s)e^{-r/\tau}\int_0^r v(r')e^{r'/\tau}dr' \\ &- u_e''(s)e^{-r/\tau}\int_0^r \Delta s(r')v(r')e^{r'/\tau}dr' + \ldots, \end{aligned} \quad (13)$$

where a prime is used to indicate the derivative with respect to its argument (i.e., $u_e'(s) = du_e(s)/ds$). Now Eq. (13) can be expressed in terms of t and x via Eqs. (5)–(7) as

$$\begin{aligned} u(t,x) &= u_e(x) - u_e'(x-\Delta x)e^{-t/\tau}\int_0^t v(t')e^{t'/\tau}dt' \\ &- u_e''(x-\Delta x)e^{-t/\tau}\int_0^t \Delta s(t')v(t')e^{t'/\tau}dt' - \ldots, \end{aligned} \quad (14)$$

where $\Delta x(t) = \int_0^t v(t')dt'$. We further expand this expression about x to find

$$\begin{aligned} u(t,x) &= u_e(x) - u_e'(x)e^{-t/\tau}\int_0^t v(t')e^{t'/\tau}dt' \\ &- u_e''(x)e^{-t/\tau}\int_0^t (\Delta x(t')v(t') - \Delta x(t)v(t'))e^{t'/\tau}dt' \\ &- \ldots. \end{aligned} \quad (15)$$

Equation (15) and our asymptotic limits serve as the basis for calculating analytical forms of statistical moments of the solution $u(t,x)$ in the next section.

III. STATISTICAL MOMENTS

We now proceed with the step-by-step derivation of the first four statistical moments in terms of statistical properties of the velocity fields and the spatial derivatives of the mean profile $\bar{u}$, using the asymptotic limit (12a) established in Subsec. II, only up to the lowest relevant order in δ_n, which is equivalent to keeping only the lowest order in $v(t)$ (keeping in mind that $\Delta x = \int_0^t v(t'')dt''$) in this case. Since $\Delta t \ll t$ and the distribution of $v(t)$ is time-independent with uncorrelated steps, the noise process is ergodic. Consequently, over a time duration $t \gg \Delta t$, the system experiences a sufficiently large number of independent random velocity steps to ensure that the time average at a fixed location is equivalent to the ensemble average. We will simply refer to such average as average in this section. For conciseness, the explicit spatial argument x in $u_e(x)$ and its derived quantities will be omitted hereafter.

A. First Moment

The first moment (average), evaluated to the lowest order in v (second order in this case), is given by taking the average of Eq. (15):

$$\bar{u} = u_e - u_e''\int_0^t (\overline{\Delta x(t')v(t')} - \overline{\Delta x(t)v(t')})e^{(t'-t)/\tau}dt', \quad (16)$$

where the bar indicates the average. We first consider the second term in the integrand, $\overline{\Delta x(t)v(t')}$. Since $t' \leq t$, somewhere within the domain of integration for $v(t'')$ in t'' in the calculation of $\Delta x = \int_0^t v(t'')dt''$, there exists a time step that includes t'. This is the only part of

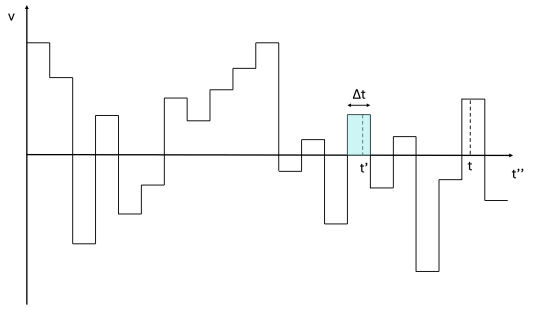


FIG. 1. A schematic of the stochastic velocity given by Eq. (11) as a function of time. A nonzero correlation between $v(t')$ and $\Delta x(t) = \int_0^t v(t'')dt''$ for $t' \leq t$ occurs only at the time step that includes $t'' = t'$, and the correlation is present for the entire time step Δt.

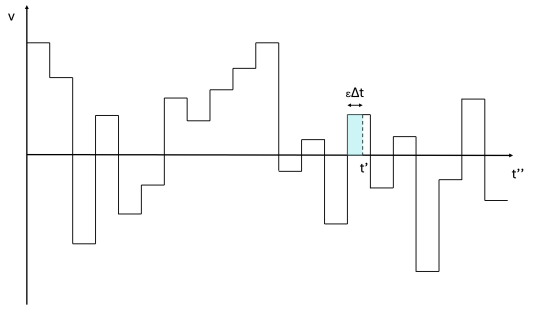


FIG. 2. A schematic of the stochastic velocity given by Eq. (11) as a function of time. A nonzero correlation between $v(t')$ and $\Delta x(t') = \int_0^{t'} v(t'')dt''$ occurs only at the last time step of the integration, the one that includes $t'' = t'$, and the correlation is present only for a fraction ϵ of the time step Δt.

$\Delta x(t)$ that is correlated with $v(t')$, and unless $t' \leq t$ is in the last time step of the integration, the entire time step is integrated in the calculation of $\Delta x(t)$ (see FIG. 1). We ignore the case where t' is in the last time step, as despite its existence, the difference makes a negligible contribution to the integral in Eq.(16) when $t \gg \Delta t$. Hence,

$$\overline{\Delta x(t)v(t')} = \overline{v(t')^2}\Delta t = \sigma_v^2 \Delta t, \tag{17}$$

where σ_v is the standard deviation of $v(t)$.

On the other hand, the first term in the integrand of Eq. (16) is given by

$$\overline{\Delta x(t')v(t')} = \epsilon(t')\sigma_v^2 \Delta t, \tag{18}$$

where $\epsilon(t')$ is the fraction of the time step that includes t'. Since the integration of $v(t'')$ in $\Delta x(t') = \int_0^{t'} v(t'')dt''$ stops at t', the nonzero correlation between $\Delta x(t')$ and $v(t')$ is present only within a fraction $\epsilon(t')$ of the time step that includes t' (see FIG. 2).

Since $\epsilon(t')$ takes purely random values between 0 and 1 at each t', its average value is 1/2. Thus, after the integration in t' in Eq. (16), we find the first moment

$$\bar{u}(x) = u_e + \frac{1}{2}u_e'' \sigma_v^2 \Delta t \tau = u_e + u_e'' \sigma_x^2, \tag{19}$$

where

$$\sigma_x^2 = \frac{1}{2}\sigma_v^2 \Delta t \tau. \tag{20}$$

Equation (19) shows that the average of u is shifted from the equilibrium profile by a quantity proportional to the correlation time, relaxation time, variance of the velocity field, and the second derivative of the equilibrium profile. Thus, a linear u_e does not shift $\bar{u}$ from u_e, but a nonlinear u_e shifts the ensemble mean by the quantity proportional to u_e'' and σ_x^2, which is the average variance of the distance traveled by the fluid during a one-dimensional random walk with a step size of $\sigma_v \Delta t$ over a time τ (i.e., half of the variance at time τ).

B. Second Moment

The second moment (variance), evaluated to the lowest order in v (second order in this case), is

$$\begin{aligned} \sigma_u^2 &= \overline{(u - \bar{u})^2} \\ &= e^{-2t/\tau} u_e'^2 \int_0^t \int_0^t \overline{v(t')v(t'')} e^{(t'+t'')/\tau} dt' dt'', \end{aligned} \tag{21}$$

where

$$\overline{v(t')v(t'')} = \sigma_v^2 \tag{22}$$

when t'' and t' are in the same time step, and zero otherwise. Thus, in the limit $\tau \ll t$,

$$\begin{aligned} \sigma_u^2 &= e^{-2t/\tau} u_e'^2 \int_0^t \sigma_v^2 \Delta t e^{2t'/\tau} dt' \\ &= \frac{1}{2} u_e'^2 \sigma_v^2 \tau \Delta t = u_e'^2 \sigma_x^2. \end{aligned} \tag{23}$$

We now use Eq. (19) to rewrite the variance in terms of $\bar{u}(x)$ and keep only the lowest order in σ_v to find

$$\sigma_u^2 = \bar{u}'^2 \sigma_x^2. \tag{24}$$

This shows that the variance is proportional to τ, Δt, and the square of the first derivative of the equilibrium profile. This is consistent with Schneider [35], where the same result was obtained with a Taylor expansion of a mean state under the assumption that the variability comes from advection of a mean state.

C. Third Moment

The third central moment μ_3 is given by

$$\mu_3 = \overline{(u - \bar{u})^3}, \tag{25}$$

where

$$u-\bar{u}=-\frac{1}{2}u_e''\sigma_v^2\Delta t\tau-u_e'e^{-t/\tau}\int_0^t v(t')e^{t'/\tau}dt' \\ -u_e''e^{-t/\tau}\int_0^t(\Delta x(t')v(t')-\Delta x(t)v(t'))e^{t'/\tau}dt'. \tag{26}$$

To the lowest order (fourth order) in v,

$$\mu_3=-3e^{-2t/\tau}u_e'^2\overline{M^2}\cdot\frac{1}{2}\sigma_v^2\tau\Delta t u_e'' \\ +3e^{-2t/\tau}u_e'^2u_e''e^{-t/\tau}\overline{M^2P}, \tag{27}$$

where

$$M=\int_0^t v(t')e^{t'/\tau}dt' \tag{28}$$

and

$$P=\int_0^t(\Delta x(t)v(t'')-\Delta x(t'')v(t''))e^{t''/\tau}dt''. \tag{29}$$

Then

$$\overline{M^2}=\frac{1}{2}\sigma_v^2\tau\Delta t e^{2t/\tau} \tag{30}$$

and

$$\overline{M^2P}=\int_{[0,t]^3}\overline{v(t_i)v(t_j)\xi(t_k)v(t_k)}e^{(t_i+t_j+t_k)/\tau}dt^3, \tag{31}$$

where $\xi(t_k)=\Delta x(t)-\Delta x(t_k)$ and $\int_{[0,t]^n}dt^n$ is a shorthand notation for $\int_0^t\int_0^t\cdots\int_0^t dt^n$ (in the present case, $dt^3=dt_idt_jdt_k$). With $\xi(t_k)=\int_0^t v(t'')dt''-\int_0^{t_k}v(t'')dt''=\int_{t_k}^t v(t'')dt''$ and Eq. (11), $\overline{v(t_i)v(t_j)\xi(t_k)v(t_k)}$ can be written as

$$\overline{v(t_i)v(t_j)[\epsilon(t_k)v(t_k)+v(t_{k+1})+\cdots+v(t)]\Delta t v(t_k)}, \tag{32}$$

where $\epsilon(t_k)$ is defined the same way as in the discussion of the first moment. Each term in this expression is of the form $\overline{v(t_1)v(t_2)v(t_3)v(t_4)}$, and it is nonzero if and only if two pairs of correlating v's are present. Furthermore, by Isserlis's theorem [36],

$$\overline{v(t_1)v(t_2)v(t_3)v(t_4)}=\overline{v(t_1)v(t_2)}\,\overline{v(t_3)v(t_4)} \tag{33}$$
$$+\overline{v(t_1)v(t_3)}\,\overline{v(t_2)v(t_4)} \tag{34}$$
$$+\overline{v(t_1)v(t_4)}\,\overline{v(t_2)v(t_3)}. \tag{35}$$

(36)

(37)

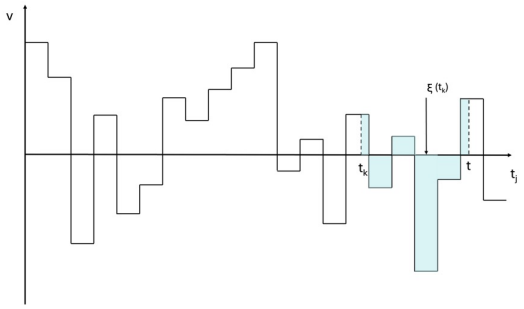


FIG. 3. A graphical representation of $\xi(t_k)$. Its correlation with $v(t_k)$ is nonzero only if $t_k\le t_j\le t$.

Hence, we find

$$\overline{M^2P}=\int_{[0,t]^3}\overline{\xi(t_k)v(t_k)}\;\overline{v(t_i)v(t_j)}e^{(t_i+t_j+t_k)/\tau}dt^3 \\ +2\int_{[0,t]^3}\overline{\xi(t_k)v(t_j)}\;\overline{v(t_i)v(t_k)}e^{(t_i+t_j+t_k)/\tau}dt^3, \tag{38}$$

where the factor of 2 in the second term comes from the symmetry between i and j. Note that,

$$\int_0^t\overline{v(t_j)\xi(t_k)}e^{(t_j+t_k)/\tau}dt_j \\ =\int_{t_k}^t\sigma_v^2\Delta t e^{(t_j+t_k)/\tau}dt_j, \tag{39}$$

as $v(t_j)$ and $\xi(t_k)$ have a nonzero correlation only if $t_k\le t_j\le t$ (see FIG. 3). Therefore,

$$\overline{M^2P}=\frac{\Delta t}{2}\int_0^t\sigma_v^2e^{2t_i/\tau}dt_i\int_0^t\sigma_v^2e^{t_k/\tau}dt_k\Delta t \\ +2\Delta t\int_0^t\sigma_v^2e^{2t_k/\tau}dt_k\int_{t_k}^t\sigma_v^2e^{t_j/\tau}dt_j\Delta t \\ =\frac{7}{12}\Delta t^2\tau^2\sigma_v^4e^{3t/\tau}. \tag{40}$$

Then Eq.(27) can be written as

$$\mu_3=3u_e'^2u_e''\Delta t^2\tau^2\sigma_v^2\left(-\frac{1}{4}+\frac{7}{12}\right) \\ =4u_e''\left(\frac{1}{2}u_e'^2\Delta t\tau\sigma_v^2\right)\cdot\left(\frac{1}{2}\Delta t\tau\sigma_v^2\right) \\ =4u_e''\sigma_u^2\sigma_x^2=\left(4\bar{u}''\frac{\sigma_x^2}{\sigma_u}\right)\sigma_u^3. \tag{41}$$

The normalized third moment (skewness) α_3 is thus given by

$$\alpha_3=\frac{\mu_3}{\sigma_u^3}=4\bar{u}''\frac{\sigma_x^2}{\sigma_u}. \tag{42}$$

The skewness is proportional to the square root of τ and Δt, and the second derivative of the equilibrium profile.

Hence, in our model, the skewness is nonzero only if u_e is nonlinear in x. The vanishing skewness with linear u_e is consistent with the idea that the variability of u comes from the advection of u_e (or the mean state); since the wind field is Gaussian, if u_e is linear in x, then symmetric velocity fluctuations yield mirror-image fluctuations in u, resulting in a zero skewness.

D. Fourth Moment

To calculate the fourth central moment , it is most convenient to first express $u(t,x)$ in terms of $\bar{u}$ instead of u_e to keep all relevant terms. Since

$$\begin{aligned} u_e &= \bar{u} - \bar{u}''\sigma_x^2, \\ u_e'(x-\Delta x) &= u_e' - u_e''\Delta x + \frac{1}{2}u_e^{(3)}\Delta x^2, \\ u_e''(x-\Delta x) &= u_e'' - u_e^{(3)}\Delta x, \end{aligned} \tag{43}$$

Eq. (15) can be written as

$$\begin{aligned} u(t,x) &= \bar{u} - \bar{u}''\sigma_x^2 \\ &- e^{-t/\tau}\bar{u}'\int v(t')e^{t'/\tau}dt' \\ &+ e^{-t/\tau}\bar{u}''\int \xi(t')v(t')e^{t'/\tau}dt' \\ &- \frac{1}{2}e^{-t/\tau}\bar{u}^{(3)}\int \left(\xi(t')^2 - 2\sigma_x^2\right)v(t')e^{t'/\tau}dt'. \end{aligned} \tag{44}$$

Therefore, the fourth central moment , evaluated to the second lowest order in v (sixth order), is

$$\begin{aligned} \mu_4 &= \overline{(u-\bar{u})^4} \\ &= e^{-4t/\tau}\bar{u}'^4\overline{M^4} + 6e^{-2t/\tau}\bar{u}'^2\bar{u}''^2\overline{M^2N^2} \\ &+ 2e^{-4t/\tau}\bar{u}'^3\bar{u}^{(3)}\overline{M^3L}, \end{aligned} \tag{45}$$

where

$$N = \sigma_x^2 - e^{-t/\tau}\int_0^t \xi(t')v(t')e^{t'/\tau}dt' \tag{46}$$

and

$$L = \int_0^t \left(\xi(t')^2 - 2\sigma_x^2\right)v(t')e^{t'/\tau}dt'. \tag{47}$$

To simplify Eq.(45), let

$$D1 = e^{-4t/\tau}\bar{u}'^4\overline{M^4}, \tag{48}$$

$$D2 = 6e^{-2t/\tau}\bar{u}'^2\bar{u}'''^2\overline{M^2N^2}, \tag{49}$$

$$D3 = 2e^{-4t/\tau}\bar{u}'^3\bar{u}^{(3)}\overline{M^3L}, \tag{50}$$

so that $\mu_4 = D1 + D2 + D3$. Then

$$\begin{aligned} D1 &= 3\bar{u}'^4e^{-4t/\tau}\int_{[0,t]^2}\overline{v(t_i)^2}\;\overline{v(t_k)^2}\Delta t^2e^{2(t_i+t_k)/\tau}dt^2 \\ &= 3\left(\frac{1}{2}\bar{u}'\tau\Delta t\sigma_v^2\right)^2 = 3\sigma_u^4, \end{aligned} \tag{51}$$

which is clearly the zeroth-order term of kurtosis. Note that,

$$\begin{aligned} e^{-t/\tau}\overline{M^2N^2} &= e^{t/\tau}\int_{[0,t]^2}\overline{v(t_i)v(t_j)}\sigma_x^4e^{(t_i+t_j)/\tau}dt^2 \\ &- 2\int_{[0,t]^3}\overline{v(t_i)v(t_j)\xi(t_k)v(t_k)}\sigma_x^2e^{(t_i+t_j+t_k)/\tau}dt^3 \\ &+ e^{-t/\tau}\int_{[0,t]^4}\overline{v(t_i)v(t_j)\xi(t_k)v(t_k)\xi(t_l)v(t_l)}e^{\sum t/\tau}dt^4, \end{aligned} \tag{52}$$

where $\sum t = t_i + t_j + t_k + t_l$. Then we find

$$D2 = -22\bar{u}'^2\bar{u}''^2\sigma_x^6 + 6\bar{u}'^2\bar{u}''^2e^{-4t/\tau}H, \tag{53}$$

where

$$H = \int_{[0,t]^4}\overline{v(t_i)v(t_j)\xi(t_k)v(t_k)\xi(t_l)v(t_l)}e^{\sum t/\tau}dt^4. \tag{54}$$

Just as in the previous case with four v_m's, $\overline{v(t_1)v(t_2)v(t_3)v(t_4)v(t_5)v(t_6)}$ is nonzero if and only if there are three pairs of two equal t_m's. Hence, using Isserlis's theorem (considering all possible combinations of three pairs), we find

$$\begin{aligned} H &= \int_{[0,t]^4}\overline{v(t_i)v(t_j)}\;\overline{\xi(t_k)v(t_k)}\;\overline{\xi(t_l)v(t_l)}e^{\sum t/\tau}dt^4 \\ &+ \int_{[0,t]^4}\overline{v(t_i)v(t_j)}\;\overline{\xi(t_k)v(t_l)}\;\overline{\xi(t_l)v(t_k)}e^{\sum t/\tau}dt^4 \\ &+ \int_{[0,t]^4}\overline{v(t_i)v(t_j)}\;\overline{\xi(t_k)\xi(t_l)}\;\overline{v(t_l)v(t_k)}e^{\sum t/\tau}dt^4 \\ &+ 2\int_{[0,t]^4}\overline{v(t_i)\xi(t_k)}\;\overline{v(t_j)\xi(t_l)}\;\overline{v(t_k)v(t_l)}e^{\sum t/\tau}dt^4 \\ &+ 2\int_{[0,t]^4}\overline{v(t_i)\xi(t_k)}\;\overline{v(t_l)\xi(t_l)}\;\overline{v(t_k)v(t_j)}e^{\sum t/\tau}dt^4 \\ &+ 2\int_{[0,t]^4}\overline{v(t_i)\xi(t_k)}\;\overline{v(t_k)\xi(t_l)}\;\overline{v(t_l)v(t_j)}e^{\sum t/\tau}dt^4 \\ &+ 2\int_{[0,t]^4}\overline{v(t_i)v(t_k)}\;\overline{\xi(t_k)\xi(t_l)}\;\overline{v(t_l)v(t_j)}e^{\sum t/\tau}dt^4. \end{aligned} \tag{55}$$

Note,

$$\begin{aligned} &\int\overline{\xi(t_k)\xi(t_l)}e^{(t_k+t_l)/\tau}dt_k \\ &= \int_0^{t_l}(t-t_l)\Delta t\sigma_v^2e^{(t_k+t_l)/\tau}dt_k \\ &+ \int_{t_l}^{t}(t-t_k)\Delta t\sigma_v^2e^{(t_k+t_l)/\tau}dt_k, \end{aligned} \tag{56}$$

as correlation between $\xi(t_k)$ and $\xi(t_l)$ with a fixed t_l is nonzero only when t'' in $\xi(t_k) = \Delta x(t) - \Delta x(t_k) = \int_{t_k}^{t}v(t'')dt''$ is in $[t_l, t]$ if $t_k \le t_l$, and is nonzero only when t'' is in $[t_k, t]$ if $t_k \ge t_l$ (see FIG. 4). The factor

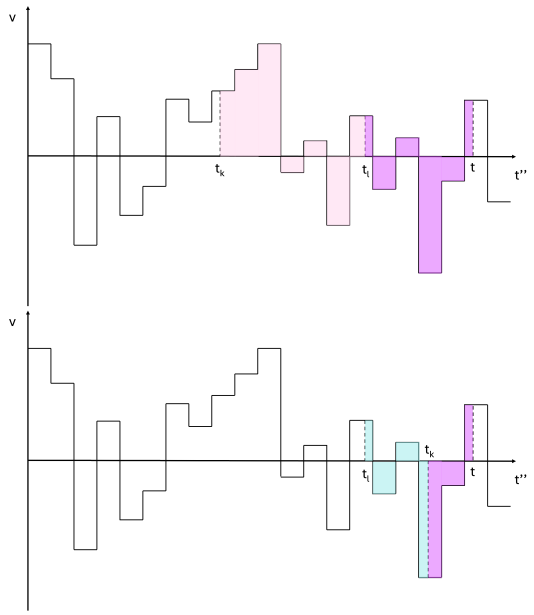


FIG. 4. A graphical representation of the correlation between $\xi(t_k)$ and $\xi(t_l)$. If we fix t_l, their correlation is nonzero when $t'' \in [t_l, t]$ if $t_k \leq t_l$, and it is nonzero when $t'' \in [t_k, t]$ if $t_k \geq t_l$. In each case, the region with a nonzero correlation is shaded with purple.

$(t-t_k)\Delta t\sigma_v^2$ comes from the random walk considerations (i.e., variance is proportional to the number of steps times the length of each step).

Using Eq. (39) and Eq. (56), Eq. (55) can be written as

$$\begin{aligned}
H &= (\Delta t\sigma_v^2)^3 \int_0^t e^{2t_i/\tau} dt_i \int_0^t \frac{1}{2} e^{t_k/\tau} dt_k \int_0^t \frac{1}{2} e^{t_l/\tau} dt_l \\
&+ (\Delta t\sigma_v^2)^3 \int_0^t e^{2t_i/\tau} dt_i \int_{t_k}^t dt_l \int_{t_l}^t e^{(t_k+t_l)/\tau} dt_k \\
&+ (\Delta t\sigma_v^2)^3 \int_0^t e^{2t_i/\tau} dt_i \int_0^t (t-t_k) e^{2t_k/\tau} dt_k \\
&+ 2(\Delta t\sigma_v^2)^3 \int_0^t e^{2t_k/\tau} dt_k \int_{t_k}^t e^{t_j/\tau} dt_j \int_{t_k}^t e^{t_i/\tau} dt_i \\
&+ 2(\Delta t\sigma_v^2)^3 \int_0^t e^{2t_k/\tau} dt_k \int_{t_k}^t e^{t_i/\tau} dt_i \int_0^t \frac{1}{2} e^{t_l/\tau} dt_l \\
&+ 2(\Delta t\sigma_v^2)^3 \int_0^t e^{2t_l/\tau} dt_l \int_{t_k}^t e^{t_i/\tau} dt_i \int_{t_l}^t e^{t_k/\tau} dt_k \\
&+ 2(\Delta t\sigma_v^2)^3 \int_0^{t_l} e^{t_k/\tau} (t-t_l) e^{(t_k+t_l)/\tau} dt_k \int_0^t e^{t_l/\tau} dt_l \\
&+ 2(\Delta t\sigma_v^2)^3 \int_{t_l}^t e^{t_k/\tau} (t-t_k) e^{(t_k+t_l)/\tau} dt_k \int_0^t e^{t_l/\tau} dt_l
\end{aligned} \tag{57}$$

Therefore (see Appendix A for detailed calculations of each term),

$$\begin{aligned}
H &= \Delta t^3\tau^3\sigma_v^6 e^{4t/\tau} \left(\frac{1}{8}+\frac{1}{8}+\frac{1}{6}+\frac{1}{6}+\frac{1}{12}+\frac{1}{3}\right) \\
&= 1 \cdot e^{4t/\tau}\Delta t^3\tau^3\sigma_v^6 = 8 \cdot \left(\frac{1}{2}\tau\Delta t\sigma_v^2\right)^3 e^{4t/\tau} \\
&= 8\sigma_x^6 e^{4t/\tau}.
\end{aligned} \tag{58}$$

Hence,

$$D2 = \bar{u}'^2\bar{u}''^2\sigma_x^6(-22+6\cdot 8) = 26\bar{u}'^2\bar{u}''^2\sigma_x^6. \tag{59}$$

To simplify D3, note that

$$\begin{aligned}
\overline{M^3 L} &= \int_{[0,t]^4} \overline{v(t_i)v(t_j)v(t_k)\xi(t_l)^2 v(t_l)} e^{\sum t/\tau} dt^4 \\
&- 2\sigma_x^2 \int_{[0,t]^4} \overline{v(t_i)v(t_j)v(t_k)v(t_l)} e^{\sum t/\tau} dt^4 \\
&= Z - 2\sigma_x^2 \cdot 3\sigma_x^4,
\end{aligned} \tag{60}$$

where

$$\begin{aligned}
Z &= 3\int_{[0,t]^4} \overline{v(t_i)v(t_j)}\ \overline{v(t_k)v(t_l)}\ \overline{\xi(t_l)^2} e^{\sum t/\tau} dt^4 \\
&+ 3\int_{[0,t]^4} \overline{v(t_i)v(t_j)}\ \overline{v(t_k)\xi(t_l)}\ \overline{\xi(t_l)v(t_l)} e^{\sum t/\tau} dt^4 \\
&+ 3\int_{[0,t]^4} \overline{v(t_i)\xi(t_l)}\ \overline{v(t_j)\xi(t_l)}\ \overline{v(t_k)v(t_l)} e^{\sum t/\tau} dt^4.
\end{aligned} \tag{61}$$

Using Eq. (39) and Eq. (56),

$$\begin{aligned}
Z &= 3(\Delta t\sigma_v^2)^3 \int_0^t e^{2t_i/\tau} dt_i \int_0^t (t-t_l) e^{2t_l/\tau} dt_l \\
&+ 3(\Delta t\sigma_v^2)^3 \int_0^t e^{2t_i/\tau} dt_i \int_{t_l}^t e^{t_k/\tau} dt_k \int_0^t \frac{1}{2} e^{t_l/\tau} dt_l \\
&+ 3(\Delta t\sigma_v^2)^3 \int_0^t e^{2t_l/\tau} dt_l \int_{t_l}^t e^{t_j/\tau} dt_j \int_{t_l}^t e^{t_i/\tau} dt_i \\
&= \left[\frac{3}{8}+\frac{3}{8}+3\left(\frac{1}{2}-\frac{2}{3}+\frac{1}{4}\right)\right]\tau^3\Delta t^3\sigma_v^6 e^{4t/\tau} \\
&= 1\cdot\tau^3\Delta t^3\sigma_v^6 e^{4t/\tau} = 8\sigma_x^6 e^{4t/\tau}
\end{aligned} \tag{62}$$

(See Appendix A for detailed calculation of each term). Therefore,

$$\begin{aligned}
D3 &= 2\bar{u}'^3\bar{u}^{(3)}(8-6)\sigma_x^6 \\
&= 4\bar{u}'^3\bar{u}^{(3)}\sigma_x^6 = 4\bar{u}'\bar{u}^{(3)}\sigma_u^2\sigma_x^4.
\end{aligned} \tag{63}$$

Finally,

$$\begin{aligned}
\mu_4 &= D1 + D2 + D3 \\
&= 3\sigma_u^4 + 26\bar{u}''^2\sigma_u^2\sigma_x^4 + 4\bar{u}^{(3)}\bar{u}'\sigma_u^2\sigma_x^4. \\
&= \left(3 + \frac{13}{8}\mu_3^2 + 4\bar{u}'\bar{u}^{(3)}\frac{\sigma_x^4}{\sigma_u^2}\right)\sigma_u^4.
\end{aligned} \tag{64}$$

(65)

To find the normalized fourth moment (kurtosis) $\alpha_4 = \mu_4/\overline{(u-\bar{u})^2}$, we first calculate the lowest-order corrections to $\overline{(u-\bar{u})^2}$. Using Eq. (44), to the fourth order in $v(t)$,

$$\begin{aligned}
&\overline{(u-\bar{u})^2} - \bar{u}^2\sigma_x^2 \\
&= \bar{u}''^2\sigma_x^4 + 2e^{-t/\tau}\bar{u}''^2\sigma_x^2\int_0^t \overline{\xi(t')v(t')}e^{t'/\tau}dt' \\
&+ e^{-2t/\tau}\bar{u}''^2\int_{[0,t]^2}\overline{\xi(t')v(t')\xi(t'')v(t'')}e^{(t'+t'')/\tau}dt'dt'' \\
&- \frac{e^{-\frac{2t}{\tau}}}{2}\bar{u}'\bar{u}^{(3)}\int_{[0,t]^2}\overline{v(t'')(\xi(t')^2 - 2\sigma_x^2)v(t')}e^{\frac{t'+t''}{\tau}}dt'dt''.
\end{aligned} \tag{66}$$

Utilizing Isserlis's theorem, Eq. (39), and Eq. (56), we find

$$\overline{(u-\bar{u})^2} - \bar{u}^2\sigma_x^2 = \bar{u}''^2\sigma_x^4 + \bar{u}'\bar{u}^{(3)}\sigma_x^4. \tag{67}$$

Therefore, kurtosis α_4 to the lowest order in $v(t)$ is given by

$$\alpha_4 = \frac{\mu_4}{\overline{(u-\bar{u})^2}} = 3 + \frac{5}{4}\alpha_3^2 - 2\bar{u}'\bar{u}^{(3)}\frac{\sigma_x^4}{\sigma_u^2}. \tag{68}$$

Note that α_3 depends on both first and second derivatives of $\bar{u}$; kurtosis depends on first, second, and third derivatives of $\bar{u}$, and scales linearly with both τ and Δt. If both second and third derivatives are zero, then excess kurtosis vanishes.

The calculations are more complicated with higher-order moments, but they can be performed in the same systematic manner.

IV. NUMERICAL VALIDATION OF THE ANALYTICAL FRAMEWORK

In this section, we compare our first four moments, (16), (24), (42), and (64), with a numerical calculation of the advection equation (1). The equilibrium function u_e is set to be a cosine function $u_e(x) = 2\cos((\pi/2)x)$, and the calculations are performed over a uniform and double-periodic domain $0 < x < 2$ with the grid size of 0.01 and the numerical timestep size of 0.01. A spatial grid refinement study and temporal numerical timestep refinement study were conducted to confirm that numerical convergence is achieved at a value 0.01 for both grid size and for numerical time step size. The stochastic velocity $v(t)$ is set by choosing random values with a Gaussian distribution at each t. Lax-Wendroff scheme is used for the integration with 5000 timesteps, which is equivalent of having $N = 5000$ realizations for calculating the statistical moments directly. We then calculate the moments using our results from $\bar{u}(x)$ and plot the moments at $0 < x < 1$.

While the analytical solution was tested across a broader range of parameters, we present two representative cases here: (i) one under ideal conditions where the theory matches the numerics exceptionally well ($\sigma_v\Delta t = 0.002$) and (ii) one where the parameters are relaxed to illustrate the expected boundaries and minor deviations of the model ($\sigma_v\Delta t = 0.01$). With a Gaussian baseline reference, uncertainties of our numerical calculations can be estimated by standard errors (SE). Since $N \gg 1$, $SE_{mean} = \sigma_u/\sqrt{N} \sim 10^{-4}$, $SE_{std} = \sigma_u/\sqrt{2N} \sim 10^{-4}$, $SE_{skewness} = \sqrt{6/N} \sim 0.035$, and $SE_{kurtosis} = \sqrt{24/N} \sim 0.069$, all of which are small compared to the peak value of each quantity by a factor of $\sim 10^{-2}$. Therefore, all moments are converged with respect to stochastic sampling

As our derivation in Sec.II, our analytical solutions of moments are for the limit where the typical distance moved by the fluid within one correlation time is small compared to the length scale of the change in $d\bar{u}/dx$, corresponding to and $\sigma_v\Delta t/((d\bar{u}/dx)/(d^2\bar{u}/dx^2)) \ll 1$.As shown in FIG. 5, our numerical solutions indeed match our analytical solutions for all four moments when $\sigma_v\Delta t/((d\bar{u}/dx)/(d^2\bar{u}/dx^2))$ is less than ~ 0.1. To show a quantitative comparison, we measure the degree of the agreement by calculating the mean absolute error normalized by the maximum magnitude of each quantity, which we call r_j, where $j \in \{\text{mean, std, skewness, kurtosis}\}$. In case (i), the average values of r_j for all x to two decimal places are 0.00, $r_{\text{std}} = 0.00$, $r_{\text{skewness}} = 0.02$, $r_{\text{kurtosis}} = 0.04$, where the values where $\delta_1 > 0.1$ (where we expect our theory deviate from numerical results) are $r_{\text{mean}} = 0.00$, $r_{\text{std}} = 0.01$, $r_{\text{skewness}} = 0.11$, $r_{\text{kurtosis}} = 0.35$. In case (ii), the average values of r_j for all x are $r_{\text{mean}} = 0.00$, $r_{\text{std}} = 0.01$, $r_{\text{skewness}} = 0.05$, $r_{\text{kurtosis}} = 0.07$, where the values where $\delta_1 > 0.1$ are $r_{\text{mean}} = 0.00$, $r_{\text{std}} = 0.02$, $r_{\text{skewness}} = 0.21$, $r_{\text{kurtosis}} = 0.31$. In both cases, the difference between theoretical and numerical values is larger when $\delta_1 > 0.1$ than overall, and the match is worse in case (ii), where the region of $\delta_1 > 0.1$ is larger. The observed differences are larger than the values of numerical uncertainty ($\sim 10^{-4}$ for mean, $\sim 10^{-3}$ for standard deviation, and $\sim 10^{-2}$ for skewness and kurtosis with our measure).

V. CONCLUSIONS

In this work, we have presented a fully analytical derivation of the single-point statistical moments for the solution of a one-dimensional nonhomogeneous advection equation governed by a random transport velocity. The framework incorporates a stochastic Gaussian transport velocity with a finite, discrete correlation time Δt and a nonzero forcing term with the linear relaxation approximation with its timescale being τ. While our methodology is applicable to moments of any arbitrary order, we have provided explicit closed-form expressions for the first four moments in the regime where the characteris-

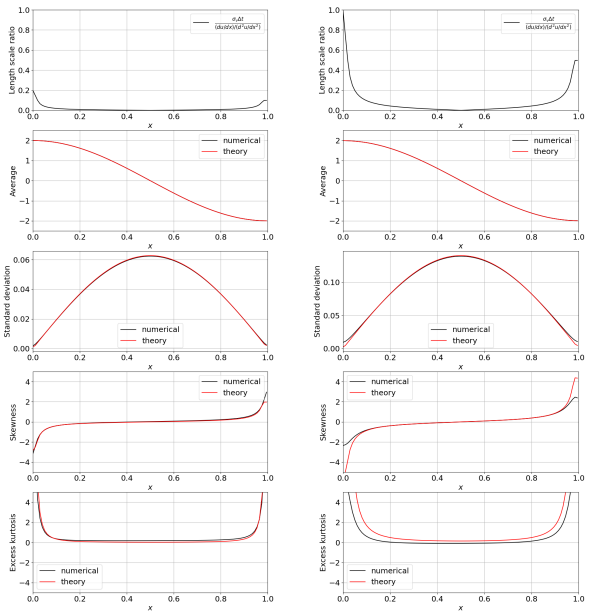


FIG. 5. Comparison between our theoretical and numerical calculation. From top: ratio of mixing length $\sigma_v\tau$ and the ratio of $\partial u/\partial x$ and $\partial^2 u/\partial x^2$ (δ_1), mean, standard deviation, skewness, and excess kurtosis of $u(t,x)$. Left: $\sigma_v\Delta t/L = 0.002$. Right: $\sigma_v\Delta t/L = 0.01$. As expected, analytical solutions match numerical simulations when $\Delta t/\tau \ll 1$ and $\sigma_v\Delta t/((d\bar{u}/dx)/(d^2\bar{u}/dx^2)) \ll 1$.

tic distance traveled by the fluid within this correlation time is short compared to the characteristic length scale of the spatial change in the equilibrium profile. We show that variance and excess kurtosis scale linearly with both the correlation and relaxation timescales, while skewness is proportional to the square root of their product. Beyond these scaling laws, our framework is connects the local temporal variability of field $u(t,x)$ at a fixed location (i.e., single-point statistical moments) to the macroscopic spatial gradients of its mean state $\bar{u}(x)$. Our expressions for the moments establish an "equation-of-state" style approach that describes the average microscale behavior of $u(t,x)$ in terms of the macroscopic quantity $\bar{u}$. Specifically, we show that non-Gaussian statistics arise directly from the nonvanishing derivatives of the underlying equilibrium profile: mean state $\bar{u}$ shifts away from the equilibrium profile u_e due to the local curvature $\bar{u}''$, the variance scales with the square of the gradient $\bar{u}'$, skewness is proportional to the second derivative $\bar{u}''$, and the excess kurtosis depends on all first three derivatives of $\bar{u}$.

The fact that the skewness is proportional to the second derivative of the mean field shows that nonlinearity of the mean profile is necessary for the presence of skewness. This is to be expected because the only physical component we consider is the advection of a scalar field by a Gaussian velocity field. Since the velocity field is symmetric, any asymmetry in the distribution of the field must arise from the asymmetry in the magnitude of positive and negative anomalies advected from the mean profile. Our result shows that a positive second derivative of the field corresponds to a positive skewness. This is consistent with the fact that such situation allows for a stronger positive anomalies to be advected (and vice versa); the sign of the second derivative thus indicates the direction of the statistical asymmetry. Furthermore, the two terms that describe excess kurtosis are proportional to the square of the skewness and to the third derivative, respectively. This means that excess kurtosis also requires nonlinearity of the field; at least one of the second or the third derivatives of the field must be nonzero.

The use of our framework is limited to the case where the characteristic length scale of the change in the mean scalar field is much larger than the characteristic length scale of the noise (i.e., the fluid does not 'feel' the change in the mean scalar field profile within one correlation time). Therefore, our theory is not applicable to physical systems where mean field profile varies sharply. It is also not applicable when the velocity of the noise is large or memory effect persist long enough for the fluid to travel far enough to feel the change in the mean field profile within a single correlation time. Moreover, since the velocity is assumed to have Gaussian statistics with piecewise constant values, our theory does not encompass non-Gaussian velocity statistics or the effect of continuous, exponentially decaying temporal correlations.

These results are applicable to physical systems characterized by advection with random transport velocity and linear relaxation in the small-displacement limit. Future efforts include generalizing the theory to two or three dimensions, and incorporating spatial dependence into the stochastic velocity field to capture more complex turbulent transport regimes, as well as applying the theory to actual physical phenomena. From a practical standpoint, this framework may be useful in multi-sector systems analysis by replacing a part of computationally heavy fluid mechanics simulations with explicit algebraic solutions.

Appendix A: Calculation of H and Z

Here, we show term-by-term calculations of H, which is given by

$$
\begin{aligned}
H &= (\Delta t\sigma_v^2)^3 \int_0^t e^{2t_i/\tau} dt_i \int_0^t \frac{1}{2} e^{t_k/\tau} dt_k \int_0^t \frac{1}{2} e^{t_l/\tau} dt_l \\
&+ (\Delta t\sigma_v^2)^3 \int_0^t e^{2t_i/\tau} dt_i \int_{t_k}^t dt_l \int_{t_l}^t e^{(t_k+t_l)/\tau} dt_k \\
&+ (\Delta t\sigma_v^2)^3 \int_0^t e^{2t_i/\tau} dt_i \int_0^t (t-t_k) e^{2t_k/\tau} dt_k \\
&+ 2(\Delta t\sigma_v^2)^3 \int_0^t e^{2t_k/\tau} dt_k \int_{t_k}^t e^{t_j/\tau} dt_j \int_{t_k}^t e^{t_i/\tau} dt_i \\
&+ 2(\Delta t\sigma_v^2)^3 \int_0^t e^{2t_k/\tau} dt_k \int_{t_k}^t e^{t_i/\tau} dt_i \int_0^t \frac{1}{2} e^{t_l/\tau} dt_l \\
&+ 2(\Delta t\sigma_v^2)^3 \int_0^t e^{2t_l/\tau} dt_l \int_{t_k}^t e^{t_i/\tau} dt_i \int_{t_l}^t e^{t_k/\tau} dt_k \\
&+ 2(\Delta t\sigma_v^2)^3 \int_0^{t_l} e^{t_k/\tau} (t-t_l) e^{(t_k+t_l)/\tau} dt_k \int_0^t e^{t_l/\tau} dt_l \\
&+ 2(\Delta t\sigma_v^2)^3 \int_{t_l}^t e^{t_k/\tau} (t-t_k) e^{(t_k+t_l)/\tau} dt_k \int_0^t e^{t_l/\tau} dt_l.
\end{aligned} \tag{A1}
$$

First term:

$$
\frac{1}{8}\Delta t^3 \tau^3 \sigma_v^6. \tag{A2}
$$

Second term:
Due to the last two integrals, this term is zero when $t_k < t_l$ and when $t_l < t_k$, which is all t. So we ignore this term.

Third term:
With integration by parts, we find

$$
\frac{1}{8}\Delta t^3 \tau^3 \sigma_v^6. \tag{A3}
$$

Fourth term:
We find

$$
\begin{aligned}
2(\Delta t\sigma_v^2)^3 \int_0^t e^{2t_k/\tau} \tau^2 (e^{t/\tau} - e^{t_k/\tau})^2 dt_k \\
= \frac{1}{6}\Delta t^3 \sigma_v^6 \tau^3.
\end{aligned} \tag{A4}
$$

Fifth term:
We find

$$
\begin{aligned}
2(\Delta t\sigma_v^2)^3 \frac{\tau^2}{2} \int_0^t e^{2t_k/\tau} (e^{t/\tau} - e^{t_k/\tau}) dt_k \\
= \frac{1}{6}\Delta t^3 \sigma_v^6 \tau^3.
\end{aligned} \tag{A5}
$$

Sixth term:
We find

$$
\begin{aligned}
2(\Delta t\sigma_v^2)^3 \int_0^t e^{2t_l/\tau} dt_l \int_{t_l}^t \tau e^{t_k/\tau} (e^{t/\tau} - e^{t_k/\tau}) dt_k \\
= \frac{1}{12}\Delta t^3 \sigma_v^6 \tau^3.
\end{aligned} \tag{A6}
$$

Seventh and eighth terms:
We find

$$
\begin{aligned}
2(\Delta t\sigma_v^2)^3 \int_0^t e^{t_l/\tau} dt_l [(t-t_l)\tau e^{t_l/\tau}(e^{t_l/\tau} - 1) \\
+ t e^{t_l/\tau} \tau (e^{t/\tau} - e^{t_l/\tau}) \\
- e^{t_l/\tau} \tau ((t_k - \tau) e^{t_k/\tau}|_{t_l}^t)]
\end{aligned} \tag{A7}
$$

$$
= \frac{1}{3}\tau^3 \Delta t^3 \sigma_v^6. \tag{A8}
$$

On the other hand, we have

$$
\begin{aligned}
Z &= 3(\Delta t\sigma_v^2)^3 \int_0^t e^{2t_i/\tau} dt_i \int_0^t (t-t_l) e^{2t_l/\tau} dt_l \\
&+ 3(\Delta t\sigma_v^2)^3 \int_0^t e^{2t_i/\tau} dt_i \int_{t_l}^t e^{t_k/\tau} dt_k \int_0^t \frac{1}{2} e^{t_l/\tau} dt_l \\
&+ 3(\Delta t\sigma_v^2)^3 \int_0^t e^{2t_l/\tau} dt_l \int_{t_l}^t e^{t_j/\tau} dt_j \int_{t_l}^t e^{t_i/\tau} dt_i.
\end{aligned} \tag{A9}
$$

The first term is identical to three times the third term for H, so the first term gives $(3/8)\Delta t^3 \tau^3 \sigma_v^6$. The second term reads

$$
\begin{aligned}
\frac{3}{2}(\Delta t\sigma_v^2)^3 \int_0^t e^{2t_i/\tau} dt_i \tau \int_0^t e^{t_l/\tau} (e^{t/\tau} - e^{t_l/\tau}) dt_l \\
= \frac{3}{8}\Delta t^3 \tau^3 \sigma_v^6.
\end{aligned} \tag{A10}
$$

Third term is identical to 3/2 times the fourth term of H, so we find $(3/2) \cdot (1/6)\Delta t^3 \tau^3 \sigma_v^6 = (1/4)\Delta t^3 \tau^3 \sigma_v^6$.

ACKNOWLEDGMENTS

This work was supported by the U.S. Department of Energy, Office of Science, Biological and Environmental Research Program, Earth and Environmental Systems Modeling, MultiSector Dynamics under Cooperative Agreement DE-SC0022141. Any opinions, findings, and conclusions or recommendations expressed in this material are those of the authors and do not necessarily reflect the views of the funding agencies. We thank Robin Stephenson for pivotal discussions and insights during a crucial stage of this research. We thank Neutrina Kircher for her unwavering canine companionship and support. During the preparation of this manuscript, the authors used Google Gemini to correct grammar and improve the flow of the text. The final text was reviewed, edited, and approved by the authors, who take full responsibility for the accuracy and integrity of the content.

Conflicts of interest

The authors have no conflicts of interest to declare that are relevant to the content of this article.

Data Availability: The numerical simulation code used to verify the analytical models and generate the plots in this study is available in Zenodo at https://doi.org/10.5281/zenodo.21197126 [37].

[1] A. P. S. Selvadurai, On the advective-diffusive transport in porous media in the presence of time-dependent velocities, Geophysical research letters **31** (2004).

[2] A. G. Hunt and M. Sahimi, Flow, transport, and reaction in porous media: Percolation scaling, critical-path analysis, and effective medium approximation, Reviews of Geophysics **55**, 993 (2017).

[3] X. Yu, K. Regenauer-Lieb, and F.-B. Tian, A hybrid immersed boundary-lattice boltzmann/finite difference method for coupled dynamics of fluid flow, advection, diffusion and adsorption in fractured and porous media, Computers & geosciences **128**, 70 (2019).

[4] M. Jochum and R. Murtugudde, Temperature advection by tropical instability waves, Journal of Physical Oceanography **36**, 592 (2006).

[5] W. H. Raymond, Moisture advection using relative humidity, Journal of Applied Meteorology **39**, 2397 (2000).

[6] C. Scott, Particle tracking simulation of pollutant discharges, Journal of environmental engineering **123**, 919 (1997).

[7] Y. Zhang, Backward particle tracking of anomalous transport in multi-dimensional aquifers, Water Resources Research **58**, e2022WR032396 (2022).

[8] S. Zhao, J. Zhou, C. Jing, and L. Li, Improved finite volume method for solving 1-d advection equation, in *Journal of Physics: Conference Series*, Vol. 1300 (IOP Publishing, 2019) p. 012075.

[9] T. J. Doerries, R. Metzler, and A. V. Chechkin, Emergent anomalous transport and non-gaussianity in a simple mobile–immobile model: The role of advection, New Journal of Physics **25**, 063009 (2023).

[10] G. Dagan, Solute transport in heterogeneous porous formations, Journal of fluid mechanics **145**, 151 (1984).

[11] R. Mauri, Heat and mass transport in nonhomogeneous random velocity fields, Physical Review E **68**, 066306 (2003).

[12] P. S. Kondratenko and L. V. Matveev, Random advection in a fractal medium with finite correlation length, Physical Review E—Statistical, Nonlinear, and Soft Matter Physics **75**, 051102 (2007).

[13] Z. Xu and A. M. Tartakovsky, Method of model reduction and multifidelity models for solute transport in random layered porous media, Physical Review E **96**, 033314 (2017).

[14] M. Linz, G. Chen, and Z. Hu, Large-scale atmospheric control on non-gaussian tails of midlatitude temperature distributions, Geophysical Research Letters **45**, 9141 (2018).

[15] T. Tamarin-Brodsky, K. Hodges, B. J. Hoskins, and T. G. Shepherd, A simple model for interpreting temperature variability and its higher-order changes, Journal of Climate **35**, 387 (2022).

[16] K. Kircher, C. Proistosescu, and R. L. Sriver, Analytical model for the higher order moments of midlatitude atmospheric temperature distributions, Geophysical Research Letters **52**, e2024GL111626 (2025).

[17] J. Giacalone and J. Jokipii, The transport of cosmic rays across a turbulent magnetic field, The astrophysical journal **520**, 204 (1999).

[18] A. D. Supanitsky, Cosmic ray propagation in the universe in presence of a random magnetic field, Journal of Cosmology and Astroparticle Physics **2021** (04), 046.

[19] A. N. Kolmogorov, Dissipation of energy in the locally isotropic turbulence, Proceedings of the Royal Society of London. Series A: Mathematical and Physical Sciences **434**, 15 (1991).

[20] R. H. Kraichnan, Anomalous scaling of a randomly advected passive scalar, Physical review letters **72**, 1016 (1994).

[21] V. Yakhot, Passive scalar advected by a rapidly changing random velocity field: Probability density of scalar differences, Physical Review E **55**, 329 (1997).

[22] G. L. Eyink, Intermittency and anomalous scaling of passive scalars in any space dimension, Physical Review E **54**, 1497 (1996).

[23] L. Wang and G. He, Solvable model for space-time correlations of passive scalars advected by turbulent flows with mean velocity, Physical Review Fluids **10**, 104607 (2025).

[24] A. Aringazin and M. Mazhitov, One-dimensional langevin models of fluid particle acceleration in developed turbulence, Physical Review E **69**, 026305 (2004).

[25] F. A. Dorini and M. C. C. Cunha, A finite volume method for the mean of the solution of the random transport equation, Applied mathematics and computation **187**, 912 (2007).

[26] F. A. Dorini, F. Furtado, and M. C. C. Cunha, On the evaluation of moments for solute transport by random velocity fields, Applied numerical mathematics **59**, 2994 (2009).

[27] L. T. Santos, F. A. Dorini, and M. C. C. Cunha, The probability density function to the random linear transport equation, Applied mathematics and computation **216**, 1524 (2010).

[28] J. Calatayud, J.-C. Cortés, F. A. Dorini, and M. Jornet, Extending the study on the linear advection equation subject to stochastic velocity field and initial condition, Mathematics and Computers in Simulation **172**, 159 (2020).

[29] M. Linz, G. Chen, B. Zhang, and P. Zhang, A framework for understanding how dynamics shape temperature distributions, Geophysical Research Letters **47**, e2019GL085684 (2020).

[30] F. A. Dorini and M. C. C. Cunha, On the linear advection equation subject to random velocity fields, Mathematics and Computers in Simulation **82**, 679 (2011).

[31] G. I. Taylor, Diffusion by continuous movements, Proceedings of the london mathematical society **2**, 196 (1922).

[32] A. F. Bennett, A lagrangian analysis of turbulent diffu-

sion, Reviews of Geophysics **25**, 799 (1987).
[33] W. Z. Daoud, J. D. W. Kahl, and J. K. Ghorai, On the synoptic-scale lagrangian autocorrelation function, J. Appl. Meteor. **42**, 318 (2003).
[34] K. L. Swanson and R. T. Pierrehumbert, Lower-tropospheric heat transport in the pacific storm track, J. Atmos. Sci. **54**, 1533 (1997).
[35] T. Schneider, T. Bischoff, and H. Płotka, Physics of changes in synoptic midlatitude temperature variability, Journal of Climate **28**, 2312 (2015).
[36] L. Isserlis, On a formula for the product-moment coefficient of any order of a normal frequency distribution in any number of variables, Biometrika **12**, 134 (1918).
[37] keikoino0212, Code for validation (2026).